

Supporting Information

Synthesis, Spectral and Redox Switchable Cubic NLO Properties of Chiral Dinuclear Iron Cyanide/Isocyanide-bridged Complexes

Xiao Ma, Chensheng Lin, Hui Zhang, Yi-Ji Lin, Sheng-Min Hu, Tian-Lu Sheng,*
and Xin-Tao Wu

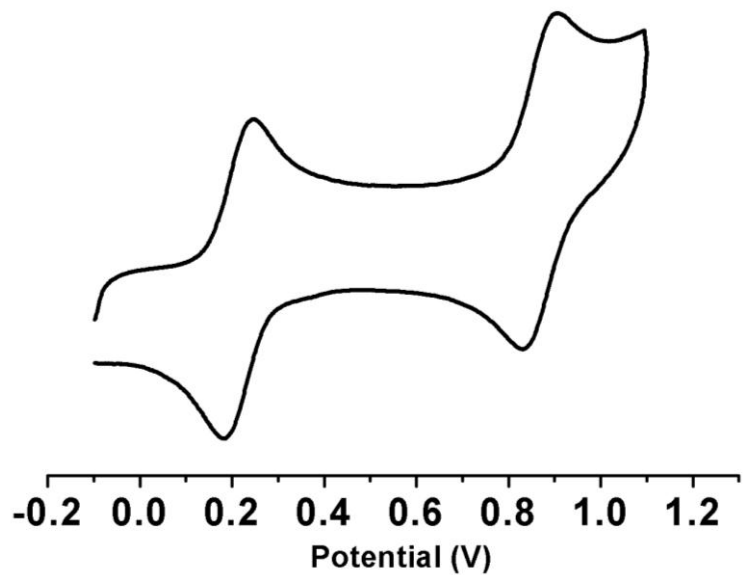


Fig. S1 Cyclic voltammogram of complex 2^+ in a 0.10 M acetonitrile solution of Bu_4NPF_6 at a scan rate of 100 mV s^{-1} .

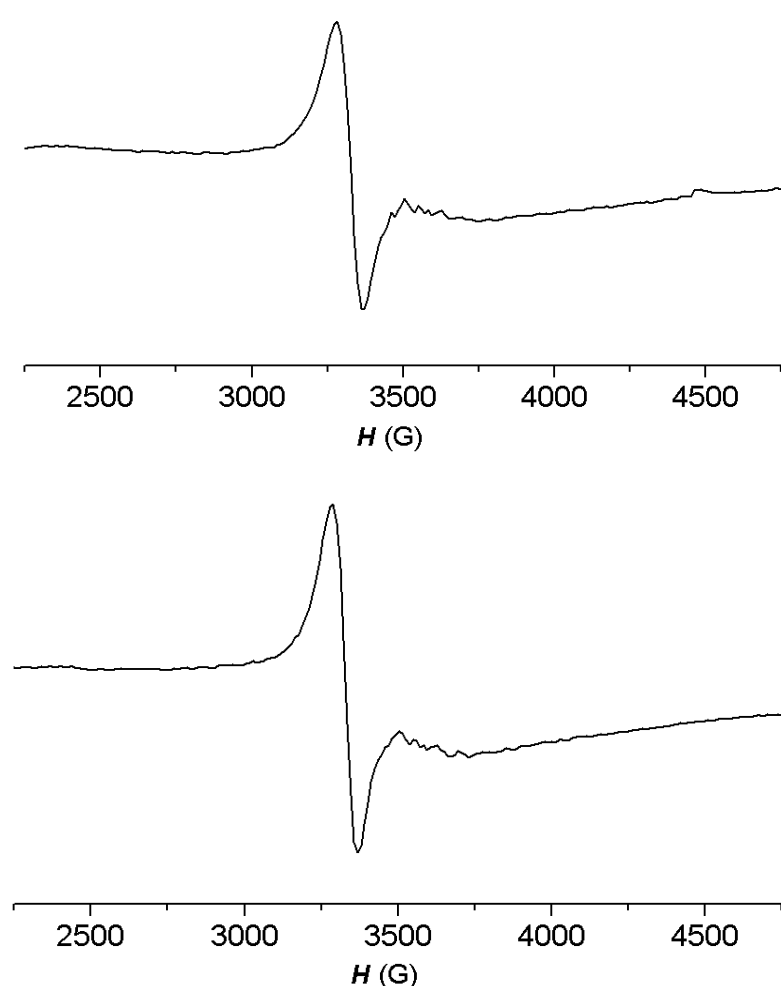


Fig. S2 X-band EPR spectra of **1**[PF₆]₂ (top) and **2**[PF₆]₂ (bottom) recorded in CH₂Cl₂ at room temperature.

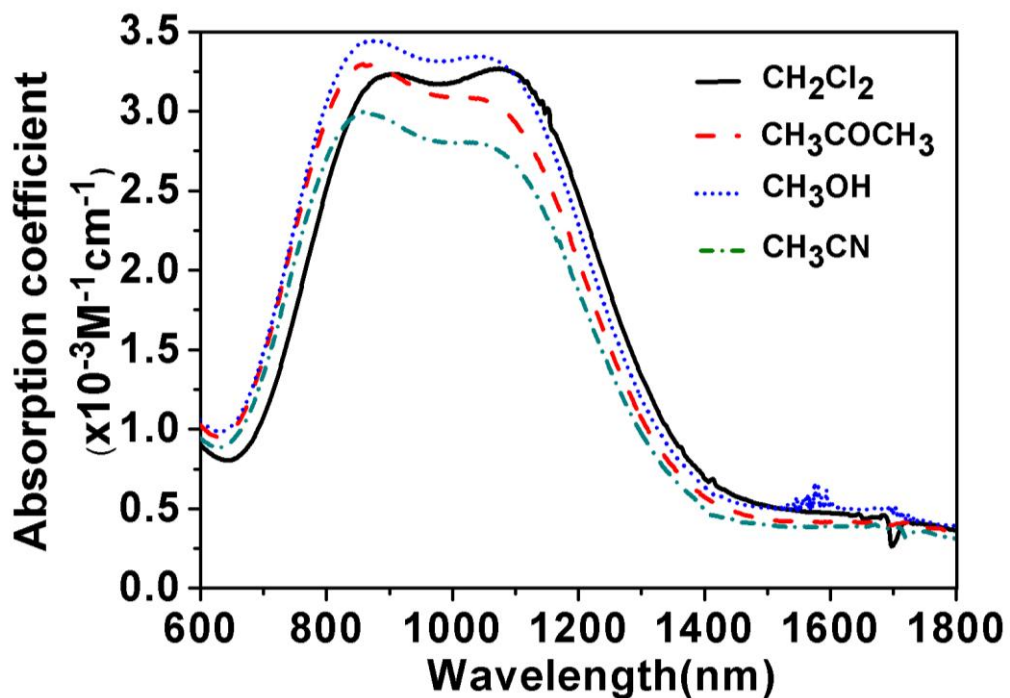


Fig. S3 IVCT band of complex $\mathbf{1}^{2+}$ in various solvents.

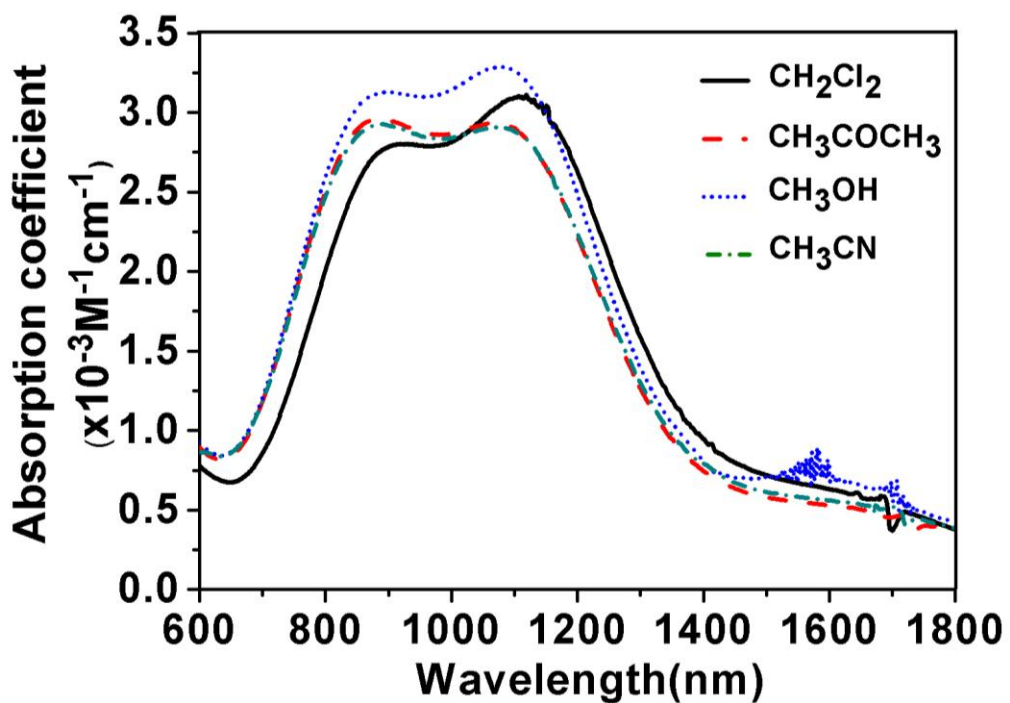


Fig. S4 IVCT band of complex $\mathbf{2}^{2+}$ in various solvents.

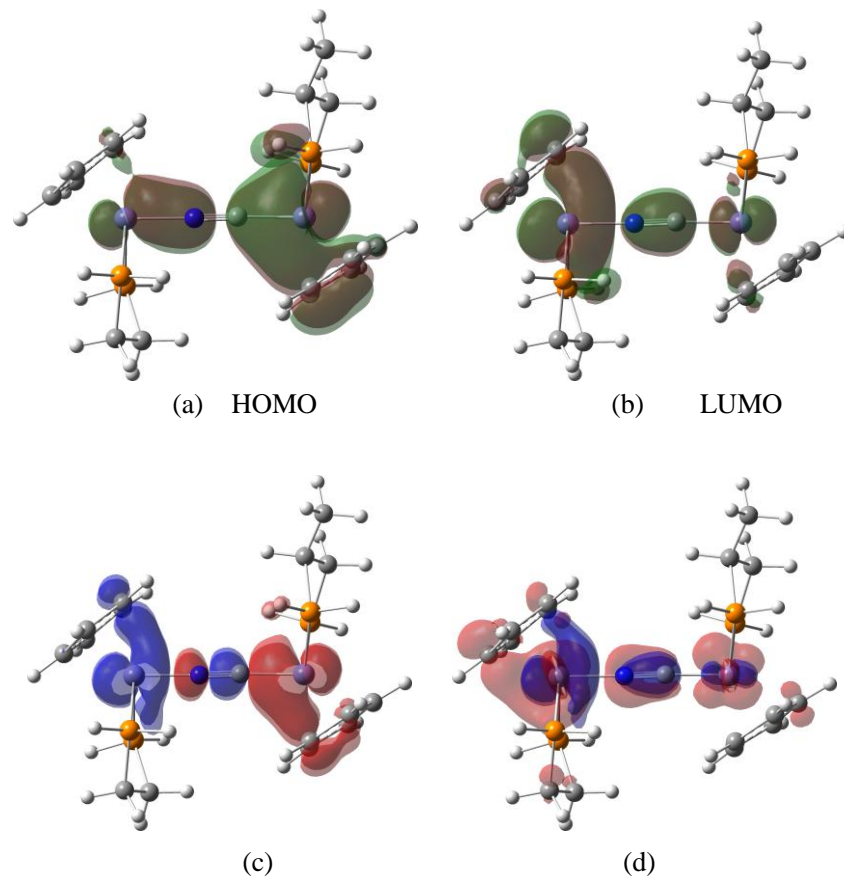


Fig. S5 Molecular orbit diagram of HOMO (a) and LUMO (b) of $\mathbf{2}^{2+}$, the isosurface value is $\pm 0.02 \text{ e } \text{\AA}^{-3}$; (c) and (d) are the deformation of charge densities of $\mathbf{2}^{2+}$ in the predicted 1.323 and 1.075 eV excitations, respectively. The blue surfaces indicate regions that have gained the charge with respect to the ground state, and the red surfaces indicate the charge depletion. The isosurface value is $\pm 0.001 \text{ e } \text{\AA}^{-3}$.

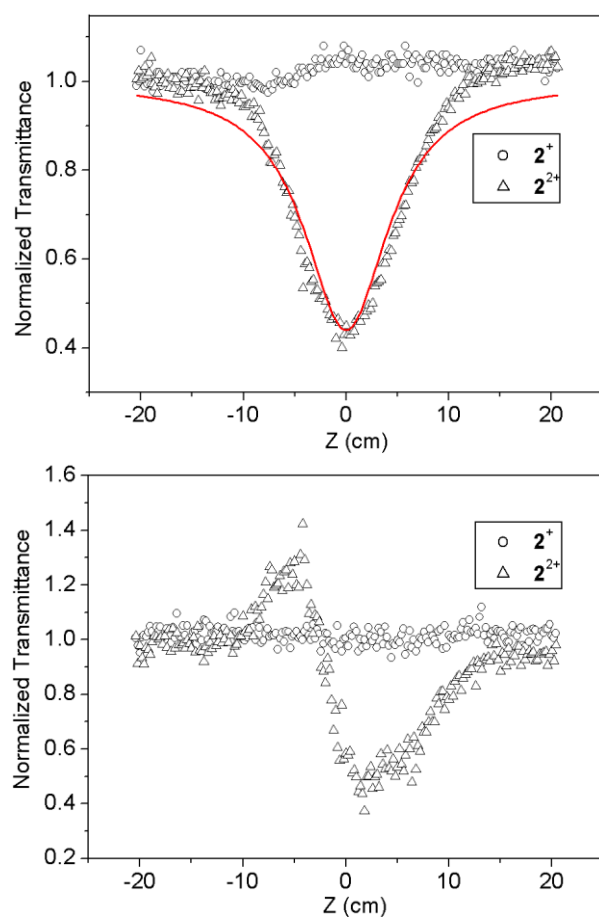


Fig. S6 Open aperture Z-scan (the nonlinear absorptive) traces and Closed aperture Z-scan (the nonlinear refractive index) traces for $\mathbf{2}^{n+}$ ($n = 1, 2$) in CH_2Cl_2 .

Table S1. Crystallographic data and structure refinements summary for complexes **1⁺** and **2⁺**

	1⁺	2⁺
formula	Fe ₂ C ₆₆ H ₆₅ F ₆ NO _{0.5} P ₅	Fe ₂ C ₆₈ H ₇₀ F ₆ NOP ₅
fw (g/mol)	1260.74	1297.80
color	dark-brown	dark-brown
T (K)	293(2)	293(2)
Crystal system	triclinic	triclinic
Space group	<i>P</i> 1	<i>P</i> 1
Z	2	2
<i>a</i> [Å]	12.049(8)	12.061(15)
<i>b</i> [Å]	12.430(7)	12.350(13)
<i>c</i> [Å]	23.884(18)	23.73(3)
α [°]	75.14(3)	74.95(5)
β [°]	77.48(3)	77.34(5)
γ [°]	66.54(3)	66.64(4)
<i>V</i> [Å ³]	3145(4)	3107(6)
Density (calcd.)[g·cm ⁻³]	1.331	1.387
μ [mm ⁻¹]	0.647	0.658
θ -range [°]	3.09, 25.50	2.02, 25.00
Index range	-14≤ <i>h</i> ≤14 -11≤ <i>k</i> ≤14 -28≤ <i>l</i> ≤28	-14≤ <i>h</i> ≤14 -13≤ <i>k</i> ≤14 -28≤ <i>l</i> ≤28
Reflections collected	18545	14773
Unique reflections	13722	13208
Observed reflections (<i>I</i> > 2 σ (<i>I</i>))	9554	8808
parameters refined	1402	1459
Flack parameter	0.11(4)	0.12(4)
Final <i>R</i> ₁ values (<i>I</i> > 2 σ (<i>I</i>))	0.0782	0.0785
Final w <i>R</i> (<i>F</i> ²) values (<i>I</i> > 2 σ (<i>I</i>))	0.1548	0.1685
Final <i>R</i> ₂ values (all data)	0.1068	0.1079
Final w <i>R</i> (<i>F</i> ²) values (all data)	0.1746	0.1900
GOOF (goodness of fit)	0.982	0.891

$$R_1 = \Sigma(|F_0| - |F_c|)/\Sigma|F_0|;$$

$$wR_2 = [\Sigma w(|F_0|^2 - |F_c|^2)^2 / \Sigma w|F_0|^2]^{1/2}$$